Computer simulation of the operation of the device for monitoring the state of high-voltage insulators during its operation

D K Zaripov, R N Balobanov and D F Zakirov

Department of Electric Stations named after V. K. Shibanov, Institute of Electric Power and Electronics, Kazan State Power Engineering University, Krasnoselskaya Str., 51, Kazan, Republic of Tatarstan, 420066, Russia

E-mail: dzaripov@list.ru

Abstract. This article presents the design and operation principle of the high-voltage isolator state indicator of the high-voltage power transmission line. The present indicator operates without the use of a separate power supply on the principle of electric field energy accumulation. The efficiency of such a device requires that as little as possible be lost during energy storage. Therefore, the development of criteria for selection of elements of the indicator circuit with minimum leakage currents is fundamental, which was one of the first tasks set during simulation. Calculations were carried out by constructing and analyzing a three-dimensional model of the insulator and solving differential equations by finite element method in the COMSOL Multiphysics software environment. The object of the study was a linear suspended insulator with polymer insulation of LK 70/35 type, designed for insulation and attachment of wires of AC overhead power transmission lines with voltage from 35 to 500 kV. Computer simulations and all calculations were made for the said insulator. On the basis of the obtained results of simulation of the insulator operation with the optical indicator installed on it, requirements to electronic components of the developed scheme were formed and corresponding components were selected.

1. Introduction

According to the brochure "Main Results of Operation of Electric Power Facilities in 2016. The results of the autumn-winter period 2016-2017”, issued by the Ministry of Energy of the Russian Federation in 2017, the number of accidents that resulted in the termination of electricity supply to consumers with a capacity of 10 MW or more due to damage to air line insulators, amounted to 12 % of the total number of accidents with such damage on overhead power transmission lines, substations and open distribution devices. If we consider only air lines, it is 22.6 %. Damage to insulators in most cases results from aging, surface contamination, manufacturing defects and accidental damage during repair work. Special place among all types of damage to isolation of overhead power transmission lines is occupied by damage to suspended polymer insulators related to their breakdown or overlap.

According to the Energy Research Institute (EPRI) in the United States, where the experience of operating polymer insulators on overhead power transmission lines is more than 30 years, over the past 10 years, US power grid enterprises have begun to experience an increasing number of polymer insulator failures on 115 and 138 kV transmission lines. EPRI studies have shown that these failures are usually associated with high electric field strength occurring near or at high voltage insulator ter-

minators. Reduction of reliability of overhead power transmission lines is caused by constant activity of electric discharges on metal terminals. Constant impact on the insulation of these corona discharges leads to cracks in the polymer shell and destruction of the end seal, so it is necessary to constantly control the condition of this type of insulators [1].

Remote isolation control methods have never been able to displace the simple visual inspection of overhead power lines and are only a supplement to it. At the same time, during visual inspection of polymer insulators it is not always possible to detect defects, as in most cases they are not visible. Consequently, there is a relevant scientific task related to the lack of effectiveness of the current methods of monitoring overhead power transmission line insulators. Its analysis revealed the need to develop and investigate new methods of insulation control with the help of devices installed on insulators, which would allow to signal their condition directly when visual inspection of overhead power transmission lines.

Installation of optical radiators signalling the presence of a defect on insulating structures in predetermined and observable places allows remote diagnosis of insulation defects under conditions of movement of the recording device. Since the position of the radiator on the insulating structure is known, algorithms for automatically detecting defects are simplified.

The principle of operation of the optical indicator is as follows: in case of violation of separate parts of the insulation structure, the distribution of the electric field along it changes. Potential difference in damaged section decreases and voltage in intact part of structure increases. Defect detection is possible by indicator illumination intensity. It depends on the drop in voltage across its electrodes and the flowing current.

Figure 1 show in a simplified way the operation of the light indicator placed in the range of the variable electric field near the insulator suspended on the metal support [2].

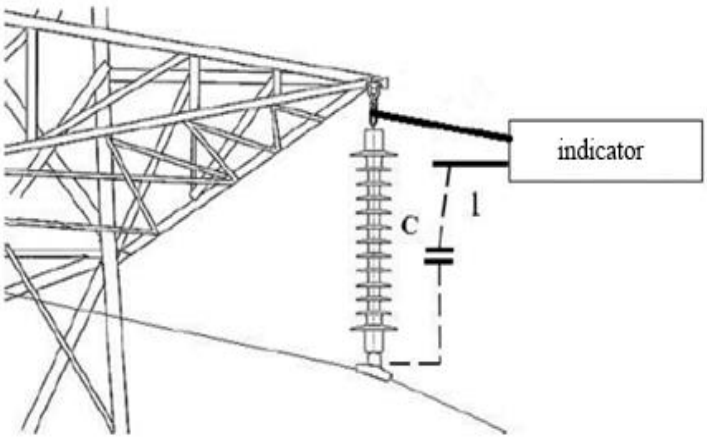

Figure 1. Indicator in the electric field near the insulator.

The figure schematically shows the electrode 1 and the electrical connection of the indicator to the metal elements of the structure. C is the capacitance of the indicator electrode relative to the high voltage portion of the structure.

The indicator diagram (figure 2) is made on the basis of dinistors [3]. A feature of this scheme is the possibility of indicating the discharges occurring in the insulation in case of damage and/or contamination. The circuit consists of two circuits. The first circuit includes the following elements: C1 capacity, R1 resistance and R2, dinistor VD6 and green LED HL1. The second circuit consists of C2 capacity, R3 resistance, VD7 dinistor and red LED HL2.

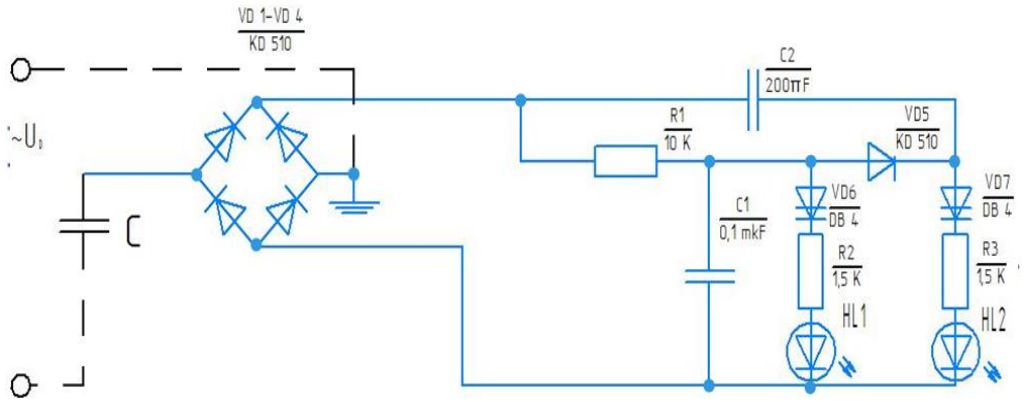

Figure 2. Dinistor-based indicator diagram.

The above-described indicator operates without using a separate power supply on the electric field energy storage principle. The efficiency of such a device requires that as little as possible be lost during energy storage. Therefore, the development of criteria for selection of elements of the indicator circuit with minimum leakage currents is fundamental. This was one of the first tasks set in the simulation.

Calculations were carried out in the COMSOL Multiphysics program [4-15] by constructing and analyzing a three-dimensional model of the LK 70/35 insulator with an optical indicator installed on it.

2. Materials and Methods

To solve this problem, a three-dimensional model of the insulator, shown in figure 3, was built in the COMSOL Multiphysics software environment.

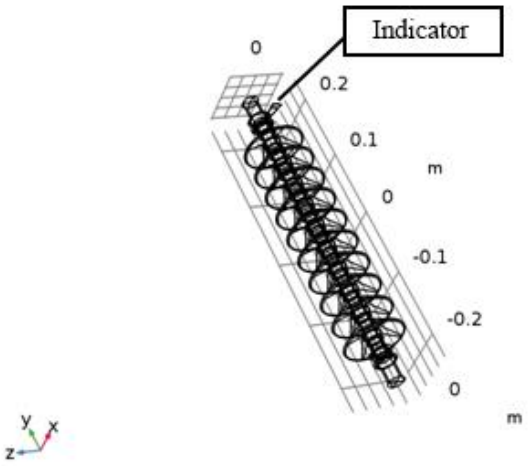

Figure 3. Geometry of three-dimensional model of LK 70/35 insulator with indicator installed at the upper end.

Figure 3 separately shows the insulator section with the indicator installed on the upper end.

A situation in which the insulator is in air was simulated, and a phase voltage of 20 kV (35 kV/1.7) is applied to both ends of the insulator, the amplitude value of which is $U_0 = 28$ kV. A parametric calculation was made where the resistance value of the R_i indicator circuit was used as a parameter. The

electronic circuit of the indicator itself was modeled by a strip of semiconductor material, the ends of which abut two electrodes, one of which is fixed on the grounded end of the insulator (figure 4).

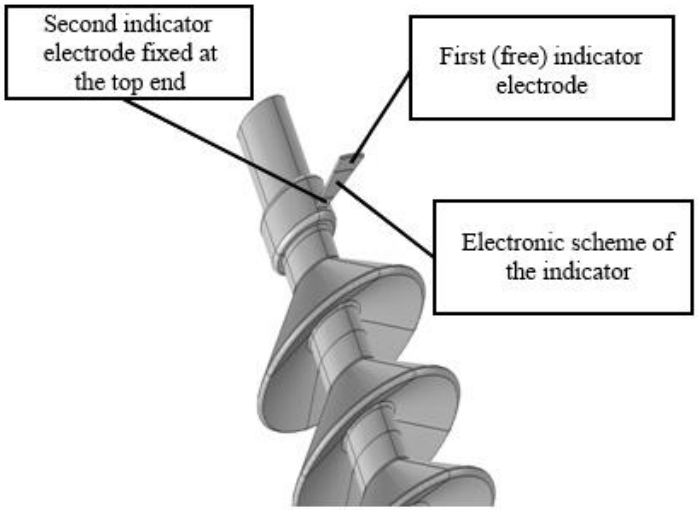

Figure 4. Indicator attached to the top end.

The variable parameter Ri was converted to the conductivity specific value G of the semiconductor strip material:

$$Ri = \frac{1}{G}\frac{l}{S} \tag{1}$$

Where l is circuit length, m; S is the section area of the strip in the middle part, m^2.

The equation by which the COMSOL Multiphysics program made calculations was derived from the continuity equation, Ohm 's law, and Gauss 's theorem. For a sinusoidal current with an angular frequency of $\omega = 2\pi f$ and an isotropic medium, these expressions will be written as:

$$J = \sigma E; \tag{2}$$

$$\nabla \cdot J = \nabla \cdot (\sigma E) = -j\omega\rho \tag{3}$$

$$\nabla \cdot D = \rho \tag{4}$$

$$E = -\nabla \cdot \mathrm{V} \tag{5}$$

$$D = \varepsilon\varepsilon_0 E \tag{6}$$

where J, E, D are vectors of current density (A/m^2), electric field intensity (V/m) and electric displacement (C/m^2), respectively; σ - specific conductivity (Cm/m); ρ – charge bulk density (C/m^3); ε – dielectric permeability of material; ε_0 - electric constant; j - imaginary unit.

After substituting the expressions for E and p into the continuity equation, the Poisson equation of the species is obtained $\nabla \cdot (-\mathrm{c}\nabla V) = \mathrm{f}$ from a set of mathematical equations solved by the COMSOL Multiphysics program:

$$\nabla \cdot (-(\sigma + j\omega\varepsilon\varepsilon_0) \cdot \nabla V) = 0 \tag{7}$$

Initial data for calculation in COMSOL Multiphysics program are given in table 1.

Table 1. Initial data for calculation in Comsol program.

Name	Value	Size	Description
l	14e-3[m]	0.014 m	Scheme length
S	1e-5[m^2]	1E−5 m²	Section area of strip (diagram) in the middle part
R	1e6[1/S]	1E6 Ω	Leakage resistance of the indicator circuit
r	R*S/l	714.29 Ω·m	Specific resistance of the indicator circuit
G	1/r	0.0014 S/m	Specific conductivity of the indicator circuit
sigma_air	0[S/m]	0 S/m	Specific conductivity of air
epsilon_air	1	1	Dielectric permeability of air
sigma_copp	5.99e7[S/m]	5.99E7 S/m	Specific conductivity of copper
epsilon_copp	1	1	Dielectric permeability of copper
sigma_al	3.77e7[S/m]	3.77E7 S/m	Specific conductivity of aluminum
epsilon_al	1	1	Dielectric permeability of aluminum
sigma_sig	1e-14[S/m]	1E−14 S/m	Specific conductivity of rubber
epsilon_sig	2.09	2.09	Dielectric permeability of rubber
sigma_gla	G	0.0014 S/m	Specific conductivity of the scheme
epsilon_gla	1	1	Dielectric permeability of the scheme
U_0	28[kV]	28000 V	Voltage amplitude at insulator
f	50[Hz]	50 Hz	Frequency

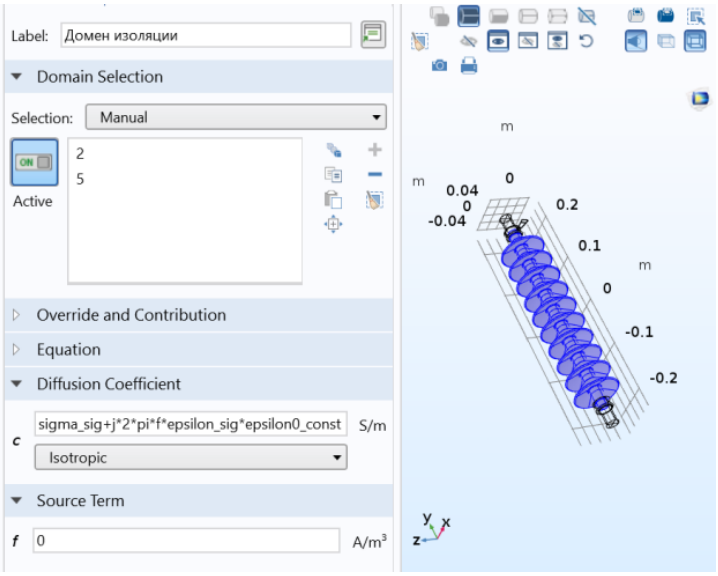

Figure 5. Set the source data for one of the domains.

The next step in simulating the operation of the insulator with an indicator installed on it for each of the regions (domains) on the example of the insulation region was to set the electrical characteristics of the materials (figure 5). Also, boundary conditions for potential, "earth" and boundary of calculation area are specified.

3. Results

Parametric calculation is made for values of leakage resistance R of electrical circuit of indicator: 1 M Ω, 10 M Ω, 100 M Ω and 500 M Ω. Figure 6 shows the voltage distribution along the insulator in pseudo-values.

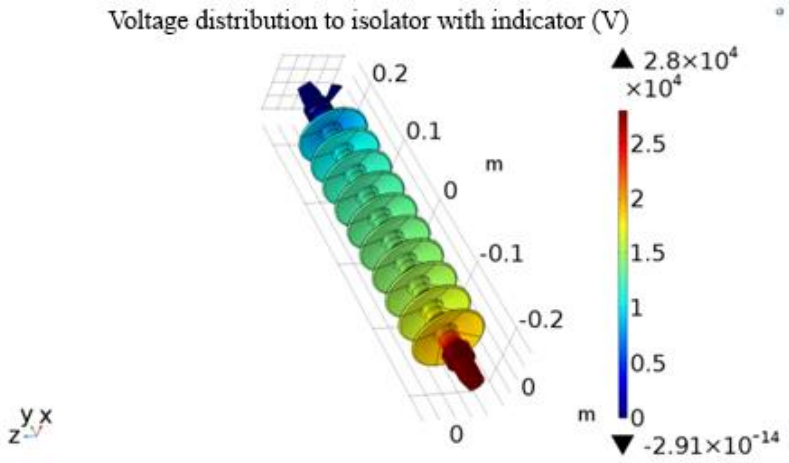

Figure 6. Voltage distribution on insulator in color.

The same graph distribution is shown in figure 7. It shows a characteristic increase in the potential gradient as it approaches the ends of the insulator.

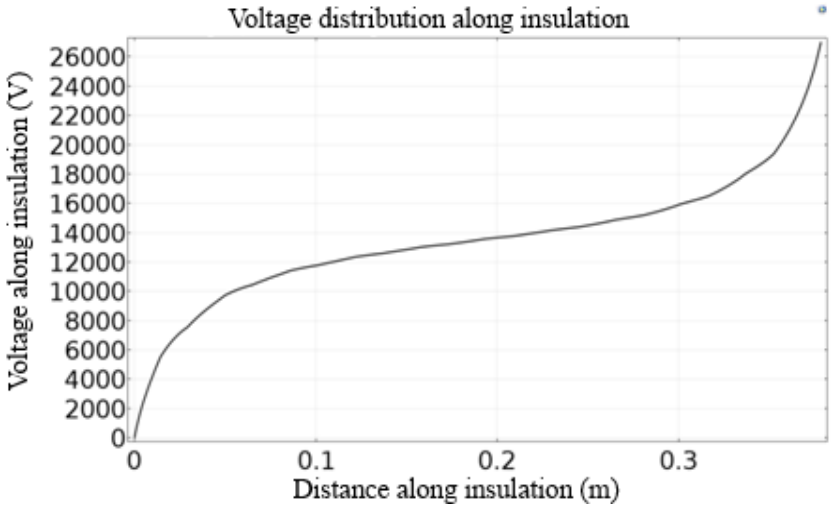

Figure 7. Voltage rise plot at insulator from grounded end to energized end.

The most important result is plotted in figure 8, which shows the potential difference between the circuit electrodes when the circuit leakage impedance changes from 1 M Ω to 500 M Ω.

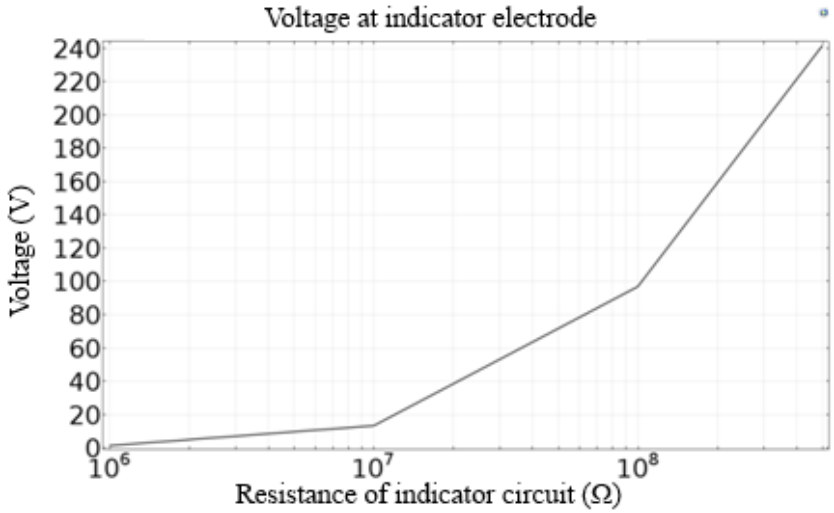

Figure 8. Dependence of amplitude value of circuit voltage on resistance of indicator circuit.

4. Discussion

From the graph shown in figure 8 it can be seen that the developed circuit based on dinistors will not work until the potential difference exceeds the voltage of dinistors actuation (~ 40 V), which can happen only if the impedance of the indicator exceeds the 20 M Ω. This important conclusion formed the basis for selecting the components and the indicator design.

5. Conclusion

In this work, first of all, the task of assessing the requirements for the design and electronic components of the indicator was solved. In addition, however, the developed model served as the basis for calculations of 35 kV insulator operation with an optical indicator, where the capabilities of the indicator were modeled and evaluated for functional purpose.

Based on the simulation results, the following components were selected: super bright LEDs (3R5 grades); dinistors (DB 4 grade), diodes (KD 510 grade) and capacitors with low leakage currents; low leakage current arrester (EC75X grade).

The most suitable emitters are ultra-bright LEDs, which have sufficient brightness to detect them from a distance of up to 50 m visually in the daytime.

References

[1] Learning from Service Experience with Composite Line Insulators URL http://www.inmr.com/learning-from-service-experience-with-composite-line-insulators/
[2] Zaripov D and Balobanov R 2016 Indikator defekta vy`sokovol`tnoj izoliruyushhej konstrukcii [High voltage insulation structure defect indicator] *E`lektrotexnika* **6** 16-21 [In Russian]
[3] Balobanov R, Zaripov D and Margulis S 2017 Ustrojstvo opticheskoj indikacii defekta vy`sokovol`tnoj izoliruyushhej konstrukcii [Device for optical indication of defect of highvoltage insulating structure] *Izvestiya vy`sshix uchebny`x zavedenij. Problemy` e`nergetiki* **4** 119-25 [In Russian]
[4] Comsol Multiphysics URL http://www.comsol.com/
[5] Bazhutin D 2015 Simulation of elastic vibrations of crane installations con-structions in comsol multiphysics package *SWVNTU* **4** 4
[6] Budko A and Vasilieva O 2014 Modelirovanie staticheskix e`lektromagnitny`x polej i raschet parametrov v comsol multiphysics [Modeling static electromagnetic fields and calculating parameters in comsol multiphysics] *Sovremennye problemy nauki i obrazovaniya* **2** 133 [In

Russian]
[7] Darrell W and Juan C 2006 *The finite element method: basic concepts and applications* (New York:CRC Press)
[8] Roger W 2009 *Multiphysics modeling using comsol: a first principles approach* (Sudbury:Jones & Bartlett Learning)
[9] Mehrzad Tabatabaian 2015 *Comsol5 for engineers* (Herndon:Mercury Learning & Information)
[10] Baker A 2012 *Finite elements: computational engineering sciences* (Chichester:John Wiley & sons LTD)
[11] William B J Zimmerman 2006 *Multiphysics modeling with finite element methods* (London: World Scientific Publishing Company)
[12] Layla S 2019 *Geometry creation and import with comsol multiphysics* (Herndon:Mercury Learning & Information)
[13] Eugenio A and David G 2015 *A practical guide to geometric regulation for distributed parameter systems* (Boca Raton:Chapman and Hall/CRC)
[14] Lennart Edsberg 2008 *Introduction to computation and modeling for differential equations* (Chichester: John Wiley & sons LTD)
[15] Darell W and Juan C 2017 *The finite element method: basic concepts and applications with matlab, maple, and comsol* (New York:CRC Press)